*Polish Journal of Chemical Technology, 14, **4**, 69 — 76, 10.2478/v10026-012-0105-2*

Simultaneous synthesis-immobilization of nano ZnO on perlite for photocatalytic degradation of an azo dye in semi batch packed bed photoreactor

Ali Khani*, Mahmoud Reza Sohrabi

Islamic Azad University, Faculty of Chemistry, North Tehran Branch, P.O. Box 66 1913674711, Tehran, Iran
**Corresponding author: e-mail: a.khani59@yahoo.com*

A novel, simple and simultaneous synthesis-immobilization of nano ZnO on perlite (nZnO-P) as a photocatalyst for photocatalytic degradation of Acid orange 7 (AO7) in aqueous solution was investigated. The effect of operational parameters such as initial dye concentration, initial pH, flow rate, photocatalyst granule size, temperature and the kinetic of the removal of AO7 in terms of the Langmuir–Hinshelwood model in a designed semi batch packed bed photoreactor connected to an on-line sampling UV-Vis spectrophotometer was studied. The results showed that AO7 removal efficiency increased with nZnO-P using the designed setup and the proposed photocatalyst was more efficient than TiO_2 as a standard catalyst. Our results confirmed the pseudo-first-order kinetics model. The values of the adsorption equilibrium constant, K_{AO7}, the kinetic rate constant of surface reaction, k_c, and the activation energy (E_a) were found to be 0.57 $(mg.l^{-1})^{-1}$, 0.41 $mg.l^{-1}.min^{-1}$ and 11.44 kJ/mol, respectively.

Keywords: Natural gas vehicle, Driving Range, Compressed Natural Gas (CNG), Thermodynamic properties, CNG fuelling station.

INTRODUCTION

Wastewater from textile, paper and some other industries contain residual dyes which are not readily biodegradable. Adsorption and chemical coagulation processes are two common techniques of wastewater treatment. However, these methods merely transfer the dyes from the liquid to the solid phase causing secondary pollution and requiring further treatment. Advanced oxidation processes (AOPs) are alternative techniques of removing dyes and many other organics in wastewater and effluents. These processes generally, involve UV/H_2O_2, UV/O_3 or UV/Fenton's reagent and etc, for the oxidative degradation of contaminants. Semiconductor photocatalysis is another developed AOP, which can be conveniently applied to remove different organic pollutants[1–5].

TiO_2 and ZnO nanopowder, especially in recent years, have been used as effective, inexpensive and nontoxic semiconductor photocatalysts for the degradation of a wide range of organic chemicals and synthetic dyes. The size of the photocatalysts is one of the most important factors. There are many comparative studies about the photocatalytic efficiency of pollutants using TiO_2 and ZnO, which emphasizes the effectiveness of TiO_2 or ZnO. In these studies, Degussa (P-25) TiO_2 (mean diameter, 25 nm) and commercial ZnO (mean diameter, 200 nm) are the most commonly used effective photocatalysts. However, the problem is the great size discrepancy of the two different kinds of photocatalysts[6–12]. ZnO nanopowder appears to be a suitable alternative to TiO_2 since its photodegradation mechanism has been proven to be similar to that of TiO_2[13,14]. ZnO nanopowder has been reported, sometimes, to be more efficient than TiO_2. Its efficiency has been reported to be particularly noticeable in the advanced oxidation of pulp mill bleaching wastewater[15,16]. The major advantage of ZnO in comparison with TiO_2 is its adsorption over a larger fraction of UV spectrum and the corresponding threshold of ZnO which is 425 nm[12,17]. In numerous investigations, an aqueous suspension of the catalyst particles in immersion or annular type photoreactor has been used. However, the use of suspensions requires separation and recycling of the ultra fine catalyst from the treated liquid and can be an inconvenient, time-consuming and expensive process[18]. In addition, the depth of penetration of UV light is limited because of strong absorption by both the catalyst particles and the dissolved organic species[19,20]. The above problems could be avoided in the photoreactors in which photocatalyst particles are immobilized onto a fixed transparent surface, such as the reactor wall or structures that are held in fixed positions in the photoreactor[21]. However, immobilization of the catalyst on a support generates a unique problem[20].

So far, vast amount of energy and efforts already have been devoted to this subject by researchers, and now it seems to be the time to find more practical ways to use the technology at industrial scale. The key to the problem of industrializing the technology seems to be simple and low cost immobilization of photocatalysts[22–25], on the solid media suitable for the treatment process.

This study is an effort to propose a novel technique for a simultaneous synthesis immobilization of ZnO nanoparticles which is more efficient and requires the minimum cost. Many techniques have been developed for immobilizing catalysts onto a solid substrate, for example, dip coating from suspension, spray coating, sputtering, sol–gel-related methods, and electrophoretic deposition. Also, different types of substrates have been tested; for example, glass beads[26], glass tubes[27], fiberglass[28], quartz[29], stainless steel[30], activated carbon[31] and silica[32]. Perlite was employed as the substrate of TiO_2 for photocatalytic degradation of Phenol[33].

It must be noted that most studies on the photodegradation of dyes involve the measurement of the concentration of the dye as a function of time by UV--Vis spectrophotometer. Therefore, the concentration of the dye should be followed by a suitable, practical,

fast responding and preferably non-destructive in situ method. The in situ measurements also allow the study of kinetics of the photodegradation process[34]. The present study envisages the simultaneous synthesis-immobilization of ZnO on the granular perlite as a new photocatalyst and its effect on the photocatalytic degradation of AO7 in designed packed bed photoreactor. The Perlite was selected as the base for ZnO for its merits including high porosity, low density, natural abundance, the absence of toxicity and low cost[33,35]. In this work, all experiments have been performed using the designed semi batch packed bed photoreactor connected to an on-line sampling UV-Vis-spectrophotometer.

MATERIALS AND METHODS

Materials

The expanded perlite used in the present study was obtained from Goohar Sahand Co. (Iran). Its chemical composition and properties are shown in Table 1. Acid Orange 7 as a target compound was purchased from Boyakhsaz Co. (Iran). Zinc Nitrate was obtained from Merck Co. (Germany). Deionized distilled water was used in all the experiments and all the experiments were repeated twice (variance (σ^2)= 0.002).

Table 1. The vehicle's Characteristics

Constituent	Percentage (Wt %)
SiO_2, Al_2O_3, K_2O, CaO, Na_2O, Fe_2O_3, MgO, MnO_2	81, 11.4, 4.3, 0.9, 0.8, 0.7, 0.6 , 0.2, 0.1
Properties	
Color	White
pH	7
Specific area	5.3 $m^2.g^{-1}$
Melting point	1573.15 K
Density	3 g/cm^3
Granule shape	Globular
Solubility in water	No soluble

Preparation of nano ZnO-Perlite

The nano particles of ZnO supported on perlite (nZnO-P) prepared from pyrolysis of the adsorbed zinc nitrate on perlite. The solution of Zn $(NO_3)_2$ was stirred with perlite in deionized distilled water for 30 min until zinc nitrate adsorbed on expanded perlite, after which perlite was filtered and washed with the deionized distilled water and then heated to 673.15 K for 1 h in air oven for pyrolysis of zinc nitrate to ZnO. To evaluate the supporting treatment, nZnO-P granules was leached twice with deionized distilled water and then dried. During treatment the tangible weight difference was not observed which indicated well-support. This method is simple, inexpensive, effective and exclusive for zinc oxide (because its salt is soluble in water that solubility is necessary in this method). For reusability evaluation of proposed photocatalyst, the used catalysts reused without any more pretreatment. By this method synthesis and immobilization of nano ZnO on perlite was performed simultaneously.

Structural characterization of perlite and Nano ZnO/ Perlite photocatalyst

The average crystallite size (D in nm) of ZnO nanoparticles was determined using X-ray Diffraction (XRD) pattern of the nZnO-P according to the Scherrer equation[12]:

$$D = k(\lambda / \beta \cos\theta)$$

where k is a constant which is 0.89, λ is the X-ray wavelength which is 0.154 nm, β is the full width at half maximum (0.0036 Radian) and θ is the half diffraction angle which is 18. The morphology of the prepared catalysts and the perlite were determined using a Leo 440i scanning electron microscope (SEM) followed by AU-coated by the sputtering method using a coater sputter SC 761.

Photocatalytic experiments

Experimental set up

In order to assess the photocatalytic degradation of Acid orange 7 (AO7), a study of reaction kinetic was carried out under UV illumination, the packed bed tubular photoreactor connected to the on-line sampling UV-Vis spectrophotometer which consisted of UV-Vis spectrophotometer, a designed absorption cell, peristaltic pump, solution reservoir, jacketed tubular pyrex (D_{out}= 5.5cm, D_{in}=2.5cm, ength= 30cm and dimension of layer of photocatalyst=3 cm) and a quartz covered UV-C lamp (8w-Philips and light intensity= 0.4 k Lux measured with a Lux-meter, Leybold-Heraeus) which is shown in Figure 1.

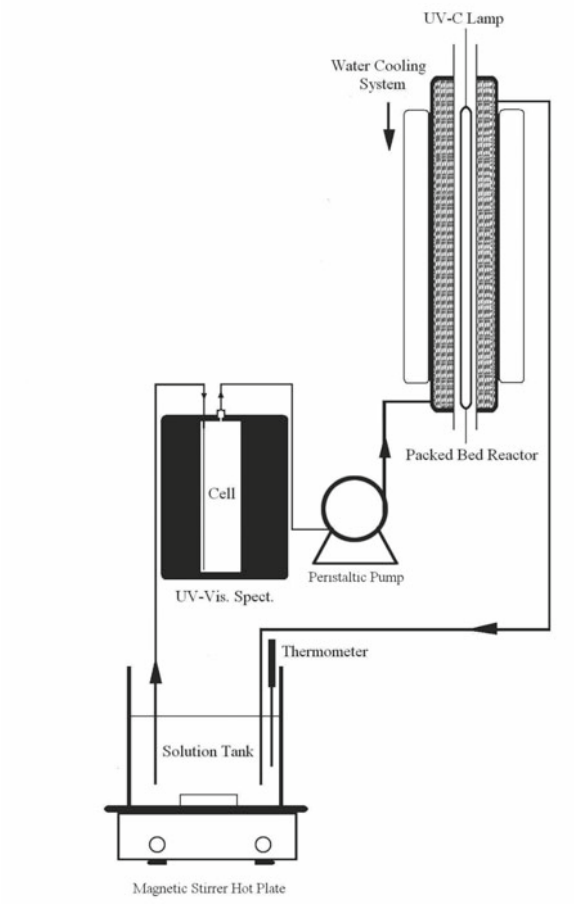

Figure 1. The schematic diagram of experimental apparatus

Procedures

For the photodegradation of AO7, a solution containing the known concentrations of dye was prepared and then 1 L of the prepared solution was transferred into a Pyrex beaker and agitated with a magnetic stirrer during the experiment. The solution was pumped with a peristaltic pump (Heidolph, PD 5001) through the circular packed bed photoreactor. To explore the effect of pH, the solution's pH was initially adjusted at desired values by adding dilute NaOH and H_2SO_4 and by controlling with a pH meter (Philips PW 9422) and the solution temperature was adjusted with a cooling system. Then the lamp was switched on to initiate the reaction. The concentration of the dye solution was determined with an on-line sampling spectrophotometer (UV-Vis Spectrophotometer, Perkin-Elmer 550 SE) system at λ_{max} =485 nm. The degree of degradation of AO7 (removal efficiency) was calculated at different time intervals using the equation given below:

$$X = \frac{C_0 - C_t}{C_0}$$

In which X is the degree of degradation, C_0 is the initial concentration of AO7, and C_t is the concentration of AO7 at time t.

RESULTS AND DISCUSSION

XRD and SEM analysis

The resulting graphs of the XRD analysis are shown in Figure 2. This figure shows clearly the same pattern for the prepared nZnO-P when compared to the standard ZnO powder[12] and the results of the calculation show that the average particle size is about 40 nm. Figure 3 shows the SEM image of the surface of the prepared catalyst. The images of perlite surface confirm the high porosity of perlite granules as a good support for the nano ZnO[33].

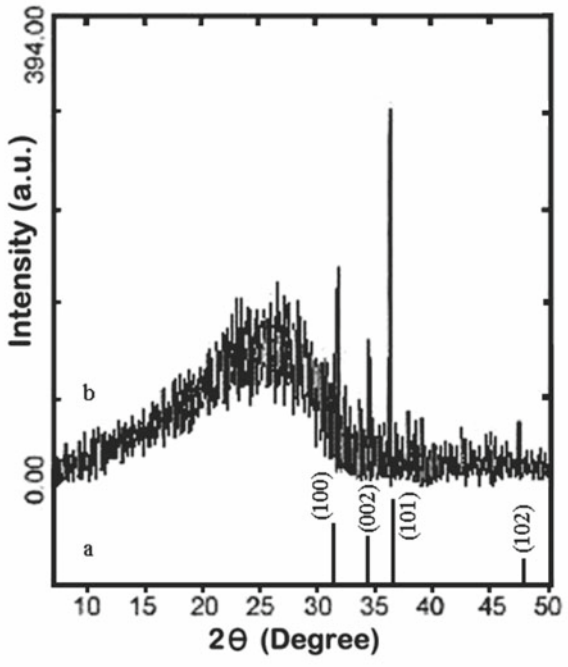

Figure 2. Standard ZnO powder diffraction pattern (a) and XRD pattern of nano ZnO immobilized on expanded perlite (b)

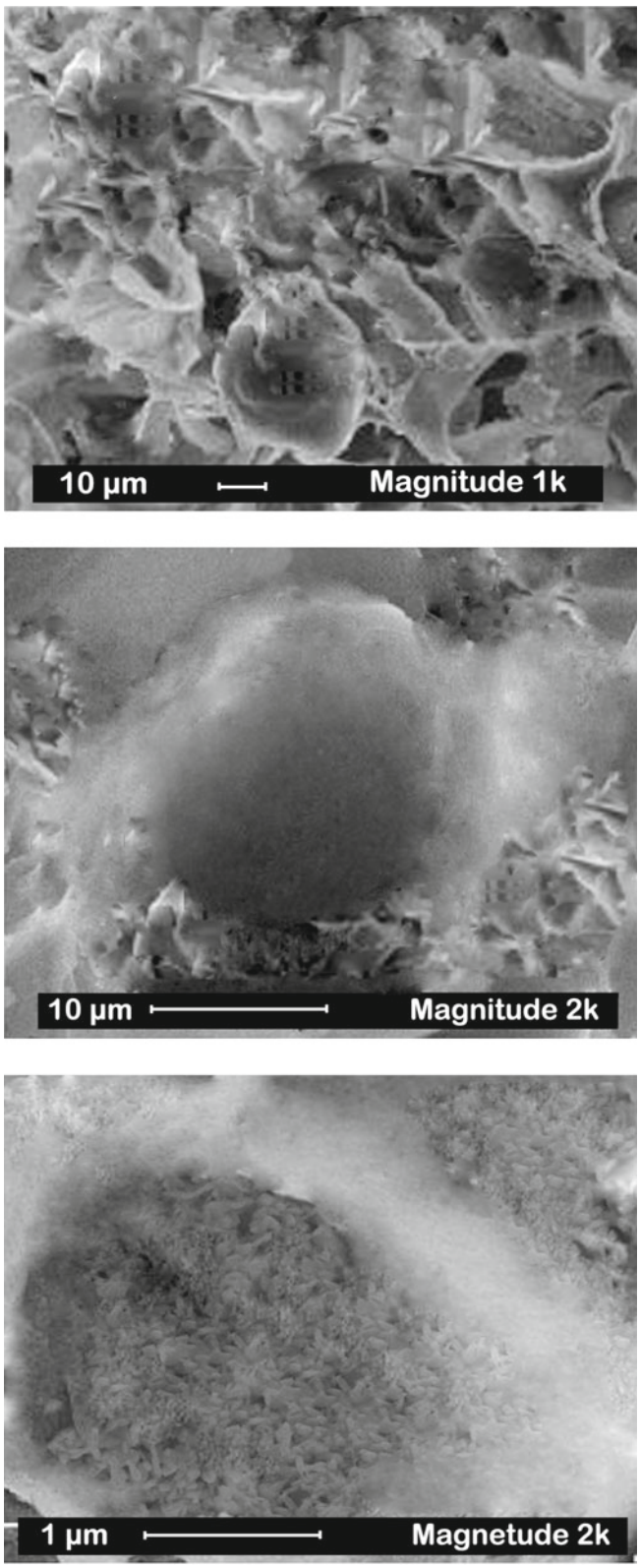

Figure 3. SEM images of perlite (a, b) and nZnO-P (c)

Control test

For the evaluation of the photocatalytic activity of the prepared photocatalyst, an experiment in basic conditions (initial concentration of AO7=25mg.l^{-1}, the weight of photocatalyst (nZnO-P)= 55g, pH =7, T=25°C, the flow rate of the solution= 150ml.min^{-1}, the granule size of photocatalyst= 4mm, the volume of solution= 1 L, and reaction time= 90 min) was designed in order to measure the degree of degradation or adsorption of AO7 on perlite and the photocatalyst in dark condition. These experiments demonstrated that both the UV light

and the photocatalyst were needed for the effective destruction of AO7 (Figure 4 (a)). The total organic carbon (TOC) analysis (Shimadzu TOC-VCSH, North America) results showed that the degradation process has occurred. The mineralization was completed in 200 min under basic conditions. Also the TiO_2, supported on perlite[33] was prepared to evaluate the potential application of the proposed photodegradation method. Fig. 4 (a) shows the comparison between the supported TiO_2 as a standard catalyst, nZnO-P and the reused photocatalyst. The results showed that n-ZnO-P was more efficient than TiO_2 and the difference between the catalyst and reused catalyst is not significant. Also, this figure shows that perlite (in darkness) and UV light do not affect the adsorption or degradation of AO7.

It has been established that the photocatalytic degradation of organic matter in the solution is initiated by photoexcitation of the semiconductor, followed by the formation of an electron–hole pair on the surface of catalyst Eq. (1). The high oxidative potential of the hole (h_{VB}^+) in the catalyst permits the direct oxidation of the organic matter (dye) to reactive intermediates Eq. (2). A more reactive hydroxyl radicals can also be formed either by the decomposition of water Eq. (3) or by the reaction of the hole with $^{\bullet}OH$ Eq. (4). The hydroxyl radical is an extremely strong, non-selective oxidant that leads to the degradation of organic chemicals[11,36].

$$ZnO + h\nu \rightarrow ZnO \quad (e_{CB}^- + h_{VB}^+) \tag{1}$$

$$h_{VB}^+ + dye \rightarrow \text{oxidation of the dye} \tag{2}$$

$$h_{VB}^+ + H_2O \rightarrow H^+ + {}^{\bullet}OH \tag{3}$$

$$h_{VB}^+ + OH^- \rightarrow {}^{\bullet}OH \tag{4}$$

Electron in the conduction band (e_{CB}^-) on the catalyst surface can reduce molecular oxygen to superoxide anion Eq. (5). This radical, in the presence of organic scavengers, may form organic peroxides Eq. (6) or hydrogen peroxide Eq. (7).

$$e_{CB}^- + O_2 \rightarrow {}^{\bullet}O_2 \tag{5}$$

$${}^{\bullet}O_2^- + dye \rightarrow dye - OO^{\bullet} \tag{6}$$

$${}^{\bullet}O_2^- + HO_2^{\bullet} + H^+ \rightarrow H_2O_2 + O_2 \tag{7}$$

Electrons in the conduction band are also responsible for the production of hydroxyl radicals, which have been indicated as the primary cause of organic photoexcitationmatter mineralization Eq. (8)[11].

$${}^{\bullet}OH + dye \rightarrow \text{degradation of the dye} \tag{8}$$

Effect of initial dye concentration

To study the effect of initial dye concentration on the photocatalytic decolorization efficiency, the experiments were carried out with initial dye concentration, varying from 15 to 55 $mg.L^{-1}$ and other parameters were in basic conditions.

The results in Figure 4 (b) show that the photocatalytic photodegradation efficiency slightly decreases with an increase in the initial amount of AO7. This may be attributed to several factors. At high dye concentration, the adsorbed dye molecules may occupy all the active sites of photocatalyst surface and this leads to decrease in degradation efficiency. It means that as the concentration of the dye increases, more and more molecules of the dye get adsorbed on the surface of the photocatalyst. Therefore, the requirement of the reactive species ($^{\bullet}OH$ and $^{\bullet}O_2^-$) needed for the degradation of the dye also increases. However, the formation of $^{\bullet}OH$ and $^{\bullet}O_2^-$ on the catalyst surface remains constant for a given light intensity, catalyst loading and duration of irradiation. Hence, the available hydroxyl radicals are inadequate for the degradation of the dye at high concentrations. Consequently, the degradation efficiency of the dye decreases as the concentration increases[37–39]. In addition, an increase in the substrate concentration can lead to the generation of intermediates, which may adsorb on the surface of the catalyst. Slow diffusion of the generated intermediates from the catalyst surface can result in the deactivation of active sites of the photocatalyst and consequently, a reduction in the degradation efficiency. In contrast, at low concentration, the number of the catalytic sites will not be a limiting factor and the rate of degradation is proportional to the substrate concentration[40]. Another reason may be due to the absorption of light photon by the dye itself leading to a lesser availability of photons for hydroxyl radical generation[39,41].

Effect of the initial pH

The pH of the solution has an important role in ions adsorption process on catalysts. The negative surface charge of perlite samples increased with an increase in pH. Electro-kinetic studies have also shown that the perlite samples have no iso-electric point and have negative zeta potential and surface charge. The variation of surface charge density of perlite samples with increasing pH can be result of the ionization of surface silanol groups [42]. The effect of pH on the photocatalytic degradation efficiency of AO7 was examined at different pH ranging from 5 to 9 in UV/nZnO-P process. The results summarized in Table 2. The results show a direct influence of the pH of the solution on the heterogeneous photocatalysis process. In alkaline solutions photodegradation efficiency was more than that in acidic solutions. It is because photodecomposition of ZnO nanoparticles takes place in acidic and neutral solutions. The photocorrosion of ZnO nanoparticles is complete at pH lower than 6. At higher pH, no photocorrosion of ZnO nanoparticles takes place. More efficient formation of hydroxyl radicals occur in alkaline solution[12]. Since, AO7 has a sulfuric group in its structure, which is negatively charged in alkaline conditions, therefore, in the alkaline solution dye may not be adsorbed onto the photocatalyst surface effectively[1,12]. In the light of the findings, it was deduced that the efficient condition for photodegradation of AO7 was neutral pH[12].

Effect of flow rate

As can be seen from Table 2, a slight improvement in photocatalytic decolourization efficiency with the increasing flow rate is observed. The reason for this is that as the dye solution flow rate is increased, the turbulence in the system is enhanced. Therefore, it may lead to the decomposition of the more adsorbed dye molecules on the surface of ZnO, thus the photocatalytic decolourization efficiency increases. The higher decolourization

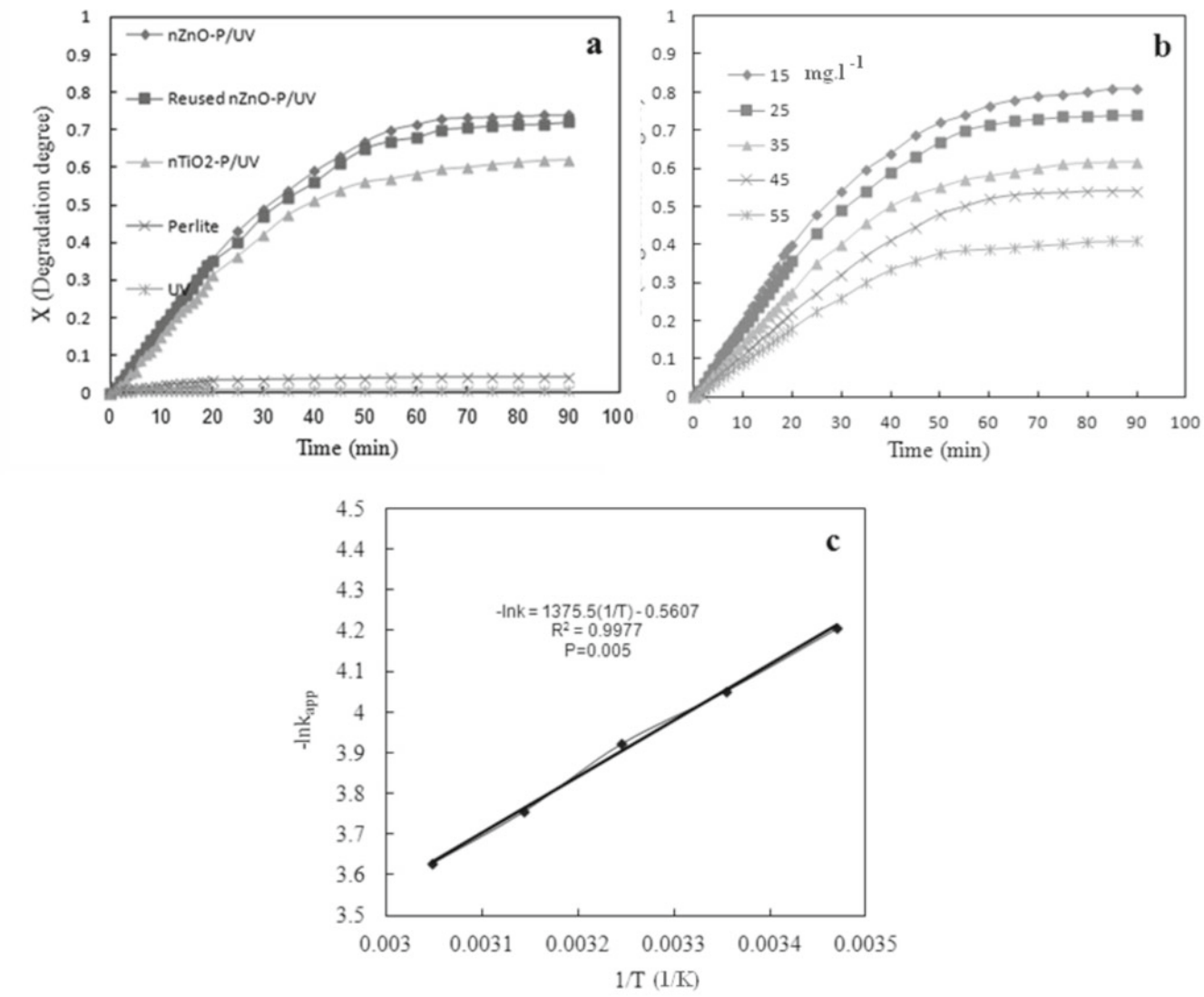

Figure 4. Effect of photocatalyst, reused photocatalyst, nano TiO_2-P, Perlite and UV light on degradation of AO7 in basic conditions (a), Effect of initial dye concentration on photodegradation efficiency of AO7 (b) and Effect of temperature on rate constant of reaction (c)

Table 2. Parameters used for calculating the average fuel power

Operational parameters	Degradation degree (X)				
pH	5	6	7	8	9
	0.091	0.191	0.74	0.49	0.37
Flow rate (ml.min^{-1})	100	125	150	175	200
	0.682	0.74	0.78	0.841	0.895
Granule size (mm)	2	4	6	8	10
	0.791	0.74	0.55	0.421	0.211
T (K)	288.15	298.15	308.15	318.15	328.15
	0.691	0.74	0.79	0.85	0.885

efficiencies at higher flow rates are also attributed to the increase in the mass transfer coefficient[43].

Effect of the photocatalyst granule size

The effect of the granule size of photocatalyst (the specific area for granule size 2, 4, 6, 8 and 10 mm was 5.5, 5.3, 5, 4.8. 4.5 and 4.3 $m^2.g^{-1}$ respectively) on the photodegradation efficiency was studied. The experiments performed with different granule size of the photocatalyst showed that the photodegradation efficiency decreases with an increase in the granule photocatalyst (Table 2). This observation can be explained in terms of availability of active sites on the catalyst surface. The total active surface area increases with decreasing the granule size.

Effect of the temperature

The changes in the dye concentration with time during the photodegradation process at each temperature are shown in Table 2. The differences in the photodegradation efficiency of the dye were small. These small differences

should originate from the effect of the energy of reaction. Fig. 4 (c) shows that the reaction rate enhances as the temperature increases from 288.15 to 328.15 K. The Arrhenius equation can be expressed as:

$$-\ln k = -\ln A + \frac{E_a}{R}\left(\frac{1}{T}\right)$$

where k = rate constant in min^{-1}, T = temperature in K[44].

The low activation energy (E_a) value 11.44 kJ/mol (calculated by figure 4 (c) results) suggests that the photodegradation of AO7 is limited by the diffusion step and an apparent rate constant reflects the rate at which AO7 molecules migrate from bulk solution to the reaction zone[44].

Kinetics of the reactions

The kinetics of the photocatalytic reactions was proposed to follow the Langmuir–Hinshelwood. The photodegradation experiments of AO7 by UV/ZnO process exhibited the pseudo-first-order kinetics with respect to the concentration of the organic compound, by using the equation of give below[12].

$$r_R = \frac{-dC_R}{dt} = \frac{k_r K C_R}{1 + K C_R}$$

where r_R is the rate of reaction (degradation of the solute R), C_R is the solute concentration, t is the time of the reaction, and k_r and K are the reaction and adsorption constants associated with the solute, respectively. When the concentration is low, the term KC_R is often negligible, and the apparent reaction rate will follow a pseudo-first-order model. Integration of the equation under this assumption with boundary conditions of $C_R = C_{R0}$ at t = 0 yields:

$$-\ln\left(\frac{C_R}{C_{R0}}\right) = k_{app} t$$

where C_{R0} is the initial substrate concentration and k_{app} is the apparent first order reaction rate. The photocatalytic reactions in many cases show this behavior. Figure 5 (a) shows the plots of the results of the photocatalytic experiments. A better criteria is to introduce a parameter known as normalized percent deviation, the lowest average absolute percent deviation (%D) or in some literature percent relative deviation modulus, P, given by the following equation[34]:

$$P = \frac{100}{N}\sum \frac{\left|y_{\exp} - y_{pred}\right|}{y_{\exp}}$$

where y_{exp} is the experimental y at any x, y_{pred} is the corresponding predicted y according to the equation under study with best fitted parameters, N is the number of observations. It is clear that the lower the P value, the better is the fit. The fit accepted to be good when P is below 5. The linear trend observed in these plots proves that the photocatalytic degradation of AO7 at the conditions of the reactions follows a pseudo-first-order kinetics. The apparent rate-constant hence calculated (slopes of the lines) are shown in Table 3.

The relationship between the initial degradation rate (r) and the initial concentration of organic substrate for heterogenous photocatalytic degradation process has been described by the Langmuir–Hinshelwood model, which can be written as follows[12]:

$$r = k_c \frac{K_{AO7}[AO7]}{1 + K_{AO7}[AO7]_0} = k_{app}[AO7]$$

$$\frac{1}{k_{app}} = \frac{1}{k_c K_{AO7}} + \frac{[AO7]_0}{k_c}$$

where K_{AO7} is the Langmuir–Hinshelwood adsorption equilibrium constant. The data reported in Table 3 were plotted in Figure 5 (b) as $1/k_{app}$ versus $[AO7]_0$. By P best fitting procedure, the values of the adsorption equilibrium constant, K_{AO7}, and the kinetic rate constant of surface reaction, k_c, were calculated [12]. The values were found to be K_{AO7} = 0.0.57 $(mg\ l^{-1})^{-1}$ and k_c = 0.41 mg l^{-1} min^{-1}.

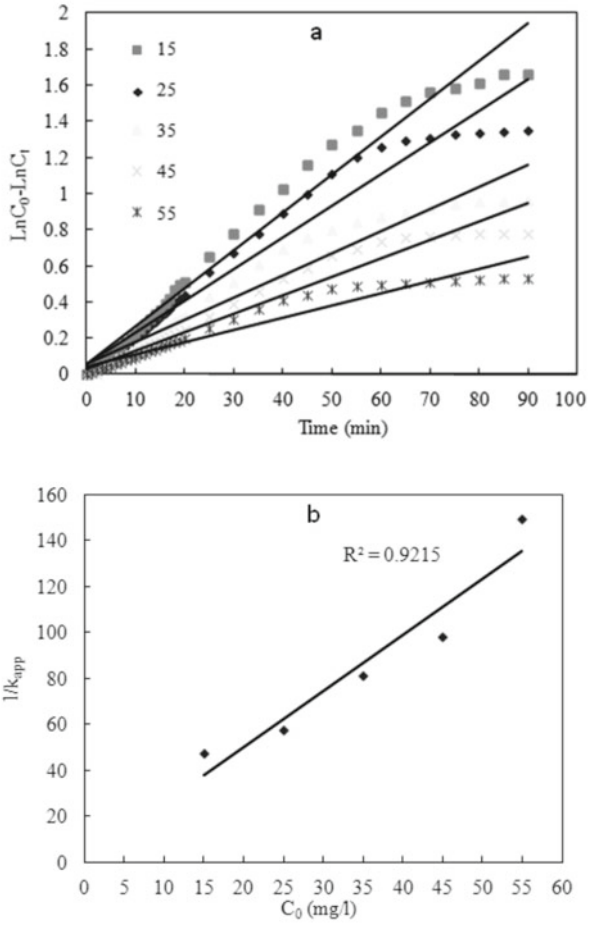

Figure 5. Determination of the pseudo-first-order kinetic rate constants, k_{app} (a) and Determination of the adsorption equilibrium constant, K_{AO7} and the second order rate constant, k_c for the Langmuir–Hinshelwood kinetic model (b)

CONCLUSIONS

In this study an easy, novel and efficient method for a simultaneous synthesis-immobilization of the nano ZnO on perlite was suggested which provided a highly

Table 3. Mole fraction of natural gas extracted from various region of Iran

$[AO7]_0$ (mg.l^{-1})	15	25	35	45	55
R^2	0.97	0.96	0.95	0.97	0.93
P	0.016	0.61	0.21	0.154	0.222
k_{app} (min^{-1})	0.021	0.0174	0.0123	0.0102	0.0067

efficient catalyst which is a cheaper and easier method for the photocatalytic oxidation of AO7 as the model pollutant. It was concluded from the XRD analysis that the simultaneous synthesis-immobilization of nanoparticles of ZnO was accomplished. SEM determination showed good uniformity of the immobilization process. The photocatalytic degradation of AO7 that confirmed with TOC analysis showed a good photocatalytic activity for the catalysts, and that designed semi batch packed bed photoreactor was efficient setup. Photolysis and adsorption were found to be negligible in the overall degradation process. The operational parameters such as initial dye concentration, pH, flow rate, photocatalyst granule size and temperature have been found to be effective in degradation process. The degradation degree (X) of photodegradation process was 0.74 under basic conditions. Perlite due to its very outstanding characteristics seems to be an ideal support for the immobilization of photocatalysts, and so can be investigated further and used for the production of commercial catalysts. The pseudo-first-order kinetics model was confirmed to satisfy these reactions using a designed packed bed photoreactor connected to an on-line sampling UV-Vis--spectrophotometer. The activation energy was 11.44 kJ/mol in temperature range of 288.15 to 328.15 K, suggesting a diffusion-controlled reaction. The values of the adsorption equilibrium constant, K_{AO7}, and the kinetic rate constant of surface reaction, k_c, were found to be 0.57 $(\text{mg l}^{-1})^{-1}$ and 0.41 $\text{mg l}^{-1}\ \text{min}^{-1}$, respectively.

Acknowledgment

The authors thank the North Tehran Branch, Islamic Azad University, Iran, for the financial support, given for this study.

LITERATURE CITED

1. Chakrabarti, S. & Dutta, B.K. (2004). Photocatalytic degradation of model textile dyes in wastewater using ZnO as semiconductor catalyst. J. Hazard. Mater. B 112(3), 269–278. DOI: 10.1016/j.jhazmat.2004.05.013.

2. Kandavelu, V., Katien, H. & Thampi, R. (2004). Photocatalytic degradation of isothiazolin-3-ons in water and emulsion paints containing nanocrystalline TiO2 and ZnO catalysts. Appl. Catal. B: Environ., 48(2), 101–111. DOI: 10.1016/j.apcatb.2003.09.022.

3. Khodja, A.A., Sehili, T., Pilichowski, J. & Boule, P. (2001). Photocatalytic degradation of 2-phenylphenol on TiO_2 and ZnO in aqueous suspension. J. Photochem. Photobiol. A: Chem., 141(2-3), 231–239. DOI: 10.1016/S1010-6030(01)00423-3.

4. Daneshvar, N., Salari, D. & Khataee, A.R. (2004). Photocatalytic degradation of azo dye acid red 14 in water on ZnO as an alternative catalyst to TiO_2. J. Photochem. Photobiol. A: Chem., 162(2-3), 317–322. DOI: 10.1016/S1010-6030(03)00378-2.

5. Zhang, D. (2010). Synthesis and characterization of ZnO--doped cupric oxides and evaluation of their photocatalytic performance under visible light. Transit. Metal Chem. 35(6), 689–694. DOI: 10.1007/s11243-010-9380-z.

6. Liu, B., Torimoto, T. & Yoneyama, H. (1998). Photocatalytic reduction of CO_2 using surface-modified CdS photocatalysts in organic solvents. J. Photochem. Photobiol. A: Chem., 113(1), 93–97. DOI: 10.1016/S1010-6030(97)00318-3.

7. Konstantinou, I., Sakellarides T., Sakkas, V. & Albanis, T. (2001). Photocatalytic degradation of selected S-triazine herbicides and organophosphorus insecticides over aqueous TiO_2 suspensions. Environ. Sci. Technol., 35(2), 398–405. DOI: 10.1021/es001271c.

8. Kwon, Y.T., Song, K.Y., Lee, W.I., Choi, G.J. & Do, Y.R. (2000). Photocatalytic behavior of WO3-loaded TiO_2 in an oxidation reaction. J. Catal., 191(1), 192–199. DOI: 10.1006/jcat.1999.2776.

9. Lin, H., Liao, S. & Hung, S. (2005). The dc thermal plasma synthesis of ZnO nanoparticles for visible-light photocatalyst. J. Photochem. Photobiol. A: Chem., 174(1), 82–87. DOI: 10.1016/j.jphotochem.2005.02.015.

10. Sakthivel, S., Neppolian, B., Shankar, M.V., Arabindoo, B., Palanichamy, M. & Murugesan, V. (2003). Solar photocatalytic degradation of azo dye: comparison of photocatalytic efficiency of ZnO and TiO_2. Sol. Energy Mater. C, 77(1), 65–82. DOI: 10.1016/S0927-0248(02)00255-6.

11. Huihu, W., Changsheng, X., Wei, Z., Shuizhou, C., Zhihong, Y. & Yanghai, G. (2004). Comparison of dye degradation efficiency using ZnO powders with various size scales. J. Hazard. Mater. B, 141(3), 645–652. DOI: 10.1016/j.jhazmat.2006.07.021.

12. Daneshvar, N., Rasoulifard, M.H., Khataee, A.R. & Hosseinzadeh, F. (2007). Removal of C.I. Acid Orange 7 from aqueous solution by UV irradiation in the presence of ZnO nanopowder. J. Hazard. Mater., 143(1-2), 95–101. DOI: 10.1016/j.jhazmat.2006.08.072.

13. Dindar, B. & Icli, S. (2001). Unusual photoreactivity of zinc oxide irradiated by concentrated sunlight. J. Photochem. Photobiol. A, 140(3), 263–268. DOI: 10.1016/S1010-6030(01)00414-2.

14. Pirkanniemi, K. & Sillanpa, M. (2002). Heterogeneous water phase catalysis as an environmental application: a review. Chemosphere, 48(10), 1047–1060. DOI: 10.1016/S0045-6535(02)00168-6.

15. Lizama, C., Freer, J., Baeza, J. & Mansilla, H. (2002). Optimized photodegradation of reactive blue 19 on TiO_2 and ZnO suspension. Catal. Today, 76(2-4), 235–246. DOI: 10.1016/S0920-5861(02)00222-5.

16. Yeber, M.C., Rodriguez J., Freer J., Baeza, J., Duran, N. & Mansilla, H. (1999). Advanced oxidation of pulp mill bleaching wastewater. Chemosphere, 39(10), 1679–1688. DOI: 10.1016/S0045-6535(99)00068-5.

17. Behnajady, M.A., Modirshahla, N. & Hamzavi, R. (2006). Kinetic study on photocatalytic degradation of C.I. Acid Yellow 23 by ZnO photocatalyst. J. Hazard. Mater. B, 133(1–3), 226–232. DOI: 10.1016/j.jhazmat.2005.10.022.

18. Ray, A. K. & Beenackers, A.A.C.M. (1997). Development of a new photocatalytic reactor for water purification. Catalysis Today, 40(1), 73–83. DOI: 10.1016/S0920-5861(97)00123-5.

19. Ray, A.K. & Beenackers, A.A.C.M. (1997). Novel swirl--flow reactor for kinetic studies of semiconductor photocatalysis. A.I.Ch.E. Journal, 43(10), 2571–2578. DOI: 10.1002/aic.690431018.

20. Chen, D. & Ray, A.K. (2001). Removal of toxic metal ions from wastewater by semiconductor Photocatalysis. Chem. Eng. Science, 56(4), 1561–1570. DOI: 10.1016/S0009-2509(00)00383-3.

21. Ray, A.K. & Beenackers, A.A.C.M. (1998). Novel photocatalytic reactor for water purification. A.I.Ch.E. Journal, 44(2), 477–483. DOI: 10.1002/aic.690440224.

22. Machado, N.R.C.F. & Santana, V.S. (2005). Influence of thermal treatment on the structure and photocatalytic activity of TiO_2 P25. Catal. Today, 107–108, 595–601. DOI: 10.1016/j.cattod.2005.07.022.

23. Gong, W.J., Tao, H.W, Zi, G.L., Tang, X.Y., Yan, Y.L., Li, B. & Wang, J.Q. (2009). Visible light photodegradation of dyes over mesoporous titania prepared by using chrome azurol S as template, Res. Chem. Intermed., 35(6), 751–760. DOI: 10.1007/s11164-009-0105-x.

24. Cheng, Y., Sun, H., Jin, W. & Xu, N. (2007). Effect of Preparation Conditions on Visible Photocatalytic Activity of Titania Synthesized by Solution Combustion Method. Chi-

nese J. of Chem. Eng., 15(2), 178–183. DOI: 10.1016/S1004--9541(07)60055-X.

25. Medina-Valtierr, J., Moctezuma, E., Sanchez-Cardenas, M. & Frausto-Reyes, C. (2005). Global photonic efficiency for phenol degradation and mineralization in heterogeneous photocatalysis. J. Photochem. Photobiol. A, 174(3), 246–252. DOI: 10.1016/j.jphotochem.2005.03.020.

26. Karches, M., Morstein, M., Rohr, P.R.V., Pozzo, R.L., Giombi, J.L. & Baltanas, M.A. (2002). Plasma-CVD-coated glass beads as photocatalyst for water decontamination. Catal. Today, 72 (3–4), 267–279. DOI: 10.1016/S0920-5861(01)00505-3.

27. Lee, J-Ch., Kim, M-S. & Kim, B.W. (2002). Removal of paraquat dissolved in a photoreactor with TiO_2 immobilized on the glass-tubes of UV lamps, Wat. Res., 36(7), 1776–1782. DOI: 10.1016/S0043-1354(01)00378-5.

28. Horikoshi, S, Watanabe, N., Onishi, H., Hidaka, H. & Serpone, N. (2002). Photodecomposition of a nonylphenol polyethoxylate surfactant in a cylindrical photoreactor with TiO_2 immobilized fiberglass cloth. Appl. Catal. B, 37(2), 117–129. DOI: 10.1016/S0926-3373(01)00330-7.

29. Martyanov, I.N. & Klabunde, K.J. (2004). Comparative study of TiO_2 particles in powder form and as a thin nanostructured film on quartz. J. Catal., 225(2), 408–416. DOI: 10.1016/j.jcat.2004.04.019.

30. Shang, J., Li, W. & Zhu, Y. (2003). Structure and photocatalytic characteristics of TiO_2 film photocatalyst coated on stainless steel webnet. J. Mol. Catal. A, 202(1–2), 187–183. DOI: 10.1016/S1381-1169(03)00200-0.

31. Ao, C.H., Lee, S.C. & Yu, J.C. (2003). Photocatalyst TiO_2 supported on glass fiber for indoor air purification: effect of NO on the photodegradation of CO and NO_2. J. Photochem. Photobiol. A, 156(1-3), 171–177. DOI: 10.1016/S1010-6030(03)00009-1.

32. Vohra, M.S. & Tanaka, K. (2003). Photocatalytic degradation of aqueous pollutants using silica-modified TiO_2. Wat. Res., 37(16), 3992–3996. DOI: 10.1016/S0043-1354(03)00333-6.

33. Hosseini, S.N., Borghei, S.M., Vossoughi, M. & Taghavinia N. (2007). Immobilization of TiO_2 on perlite granules for photocatalytic degradation of phenol. Appl. Catal. B: Environmental, 74(1-2), 53–62. DOI: 10.1016/j.apcatb.2006.12.015.

34. Daneshvar, N., Aber, S., Khani, A. & Khataee, A.R., (2007). Study of imidaclopride removal from aqueous solution by adsorption onto granular activated carbon using an on-line spectrophotometric analysis system. J. Hazard. Mater., 144(1–2), 47–51. DOI: 10.1016/j.jhazmat.2006.09.081.

35. Erdem, T.K., Meral, C., Tokyay, M. & Erdogan, T.Y. (2007). Use of perlite as a pozzolanic addition in producing blended cements. Cem. Concr. Compos., 29(1), 13–21. DOI: 10.1016/j.cemconcomp.2006.07.018.

36. Zhang, D. (2012). Structural, optical, electrical, and photocatalytic properties of manganese doped zinc oxide nanocrystals. Russ. J. Phys. Chem. A. 86(1), 93–99. DOI: 10.1134/S0036024412010086.

37. Kesraoui-Abdessalem, A., Oturan, N., Bellakhal, N., Dachraoui, M. & Oturan, M.A. (2008). Experimental design methodology applied to electro-Fenton treatment for degradation of herbicide chlortoluron. Appl. Catal. B, 78(3-4), 334–341. DOI: 10.1016/j.apcatb.2007.09.032.

38. Bahnemann, W., Muneer, M. & Haque, M.M. (2007). Titanium dioxide-mediated photocatalysed degradation of few selected organic pollutants in aqueous suspensions, Catal. Today, 124(3-4), 133–148. DOI: 10.1016/j.cattod.2007.03.031.

39. Khataee, A.R., Zarei, M., Fathinia, M. & Khobnasab Jafari, M. (2011). Photocatalytic degradation of an anthraquinone dye on immobilized TiO_2 nanoparticles in a rectangular reactor: Destruction pathway and response surface approach. Desalination, 268(1-3), 126–133. DOI: 10.1016/j.desal.2010.10.008.

40. Selvam, K., Muruganandham, M., Muthuvel, I. & Swaminathan, M. (2007). The influence of inorganic oxidants and metal ions on semiconductor sensitized photodegradation of 4-fluorophenol. Chem. Eng. J., 128(1), 51. DOI: 10.1016/j.cej.2006.07.016.

41. Damodar, R.A. & Swaminathan, J.T. (2007). Decolourization of reactive dyes by thin film immobilized surface photoreactor using solar irradiation. Sol. Energy, 81(1), 1–7. DOI: 10.1016/j.solener.2006.07.001.

42. Ghassabzadeh, H., Torab-Mostaedi, M., Mohaddespour, A., Ghannadi Maragheh, M., Ahmadi, S.J. & Zaheri, P. (2010). Characterizations of Co (II) and Pb (II) removal process from aqueous solutions using expanded perlite. Desalination, 261(1-2), 73–79. DOI: 10.1016/j.desal.2010.05.028.

43. Dijkstra, M.F.J., Panneman, H.J., Winkelman, J.G.M., Kelly, J.J. & Beenackers, A.A.C.M. (2002). Modeling the photocatalytic degradation of formic acid in a reactor with immobilized catalyst. Chem. Eng. Sci., 57(22-23), 4895–4907. DOI: 10.1016/S0009-2509(02)00290-7.

44. Behnajady, M.A., Modirshahla, N., Shokri, M. & Vahid, B. (2008). Effect of operational parameters on degradation of Malachite Green by ultrasonic irradiation. Ultrasonics Sonochemistry, 15(6), 10091014. DOI: 10.1016/j.ultsonch.2008.03.004.